

## Relation between stable orbits and quantum transmission resonance in ballistic cavities

Y. Takagaki and K. H. Ploog

*Paul-Drude-Institut für Festkörperelektronik, Hausvogteiplatz 5-7, D-10117 Berlin, Germany*

(Received 30 March 2000)

Classical and quantum-mechanical transport properties in chaotic cavities are investigated to establish a link between them. Because of the stickiness at the boundary between stochastic seas and islands of regular orbits in phase space, classical trajectories spend a long time in the vicinity of a few regular orbits. The trapping results in an exclusive excitation of these stable orbits even when the cavity is terminated by classical leads. The wave-function pattern at quantum transmission resonances is found to be identical with one of the stable orbits. The correspondence implies that the transmission resonance takes place when the stable orbit satisfies Bohr and Sommerfeld's quantization rule, and hence explains why conductance fluctuations in ballistic cavities contain only several frequency components.

PACS number(s): 05.45.Pq, 73.20.Dx, 73.23.Ad

One of the striking features of the quantum transport properties in microstructures is the transmission resonance. When the Fermi energy  $E_F$  coincides with a quasibound state level in a cavity, the conductance is suppressed or enhanced, or exhibits both effects with a narrow energy separation. If the cavity size is comparable to the Fermi wavelength  $\lambda_F$ , the probability density  $|\psi(\mathbf{r})|^2$  at the transmission resonance exhibits a simple standing wave pattern. As the quasibound states originate from zero-dimensional (0D) states in the cavity, the number of peaks and nodes increases with the index number of the transmission resonance [1]. This standing wave pattern has no classical counterpart as the probability density is anticipated to be uniform in the classical dynamics.

When the cavity is much larger than  $\lambda_F$ , the standing wave pattern involves many peaks and nodes. As a consequence, one may expect that  $|\psi|^2$  is uniform on length scales larger than  $\lambda_F$ . In contrast to this expectation, the probability density is often characterized by a large scale structure [2]. This quantum eigenstate pattern, which evolves out of the large degree of freedom of the system, arises as  $|\psi|^2$  is enhanced near classical regular orbits [3,4].

When an isolated cavity is opened to the external environment, the 0D levels are nonuniformly broadened in energy. States that couple strongly to the leads are strongly broadened, while those that couple only weakly are not. If the transport properties reflect the fluctuations in the density of states (DOS), the orbits that correspond to those states of the cavity that survive the introduction of external coupling may give rise to measurable transport signatures. Recently, it has become possible to experimentally investigate the quantum transmission properties in ballistic cavities [5–7]. A Fourier analysis of magnetoconductance fluctuations, which arise from the quantum interference effects, has revealed that the spectrum is dominated by a small number of frequency components, i.e., the conductance fluctuations are quasiperiodic [7]. The wave-function scarring has been speculated to be associated with this quasiperiodic nature of the conductance fluctuations [5]. However, it has remained unclear which regular orbit emerges as a “scar” pattern. To explain the wave-function scarring, it was proposed that the quantum-

mechanical injection of electrons into the cavity allows only a few cavity states to be excited because of the collimation effect [8,9].

In this paper, we demonstrate that only one or a few regular orbits can be strongly excited even when the coupling of the cavity with the leads is classical. The exclusive excitation of specific orbits originates from sticking in the mixed phase space of chaotic dynamics. It is important to recognize the fact that there are two classes of chaotic dynamics, namely, hyperbolic and nonhyperbolic. In the hyperbolic case, all classical trajectories are unstable and the probability  $P(t)$  of an electron remaining in the cavity for a time longer than  $t$  decays exponentially with  $t$ . In the nonhyperbolic case, the classical phase space contains stable orbits and the probability distribution is given by a power law. The classical scattering associated with the cavity geometries that are typically employed in experiments is hyperbolic when the electron confinement is by hard walls. However, it is nonhyperbolic in soft-wall cavities. In experimental situations, the classical dynamics is more likely nonhyperbolic than hyperbolic because of the inevitability of softening of confinement potentials in gate-defined devices. In addition, the magnetic field, which is applied to induce the conductance fluctuations, can give rise to a mixed phase space. We show that the scarlike wave-function pattern at the transmission resonance is nothing but the stable orbits that are favored by the underlying classical dynamics.

Ketzmerick [10] has investigated the statistical properties of the conductance fluctuations. It was shown using a semiclassical approximation that the fluctuations in cavities with a mixed phase space are fractal. We demonstrate that individual features of the conductance fluctuations are directly related to regular orbits.

We first examine the classical dynamics in a soft-wall cavity to demonstrate the strong excitation of stable orbits [11]. We employ a cavity potential, the boundary of which at the Fermi level is given by

$$y_B(x) = \pm (W/8)[3 + \cos(2\pi x/L)] \quad (|x| < L/2), \quad (1)$$

where  $W$  and  $L$  are the width and the length of the cavity. The plus and minus signs refer to the upper and lower

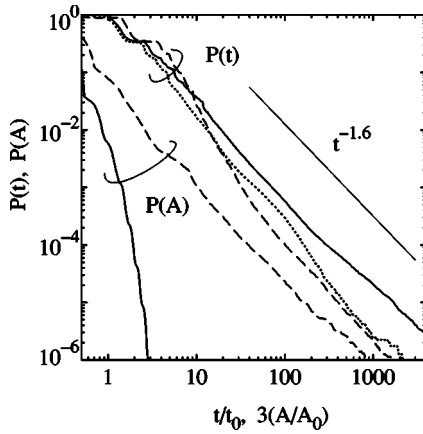


FIG. 1. Probability  $P(t)$  of electrons staying in a cavity with  $L=1.4W$  for a time longer than  $t$  and probability  $P(A)$  of the enclosed area being larger than  $A$ . Here,  $t_0=L/v_F$  and  $A_0=LW$ . The probability distributions at  $B=0$  and  $2B_0$  are shown by the solid and dashed lines, respectively. The dotted line shows  $P(t)$  in a hard-wall cavity at  $B=0$ . The thin solid line shows that the power-law exponent is  $\beta=1.6$ .

boundaries, respectively. The cavity is connected at each end to a lead with width  $W/2$ . We assume parabolic walls of width  $W/4$ , unless stated otherwise. Throughout this paper, we choose  $L=1.4W$ .

Figure 1 shows  $P(t)$  and the probability  $P(A)$  that the area enclosed by the trajectories is larger than  $A$ . Here,  $t$  and  $A$  are normalized by  $t_0=L/v_F$ , with  $v_F$  being the Fermi velocity, and  $A_0=LW$ , respectively. For soft confinement,  $P(t)$  exhibits a power-law behavior with the exponent  $-1.6$ . In the presence of a magnetic field  $B$ , the dynamics is modified to be more regular. Consequently,  $P(t)$  deviates from the power-law behavior for short trajectories [12]. However, the exponent for long trajectories remains almost unchanged. Despite the power-law behavior of  $P(t)$ ,  $P(A)$  at  $B=0$  decays exponentially with  $A$ . This is plausibly because of the wide lead, which enlarges the volume of direct trajectories in phase space. However,  $P(A)$  is given by a power law as soon as the direct trajectories are suppressed for  $B/B_0=W/r_c>0.05$ , where  $B_0=mv_F/eW$  and  $r_c=mv_F/eB$  is the cyclotron radius. The exponent is again nearly independent of  $B$  and almost identical to that of  $P(t)$ . The rapid achievement of the power law in  $P(A)$  suggests that the lead alignment is not crucial for the chaotic dynamics except at  $B=0$  or, perhaps, when the collimation is exceptionally strong. Short trajectories, however, are significantly influenced by the lead configuration.

In Fig. 2(a), we show the Poincaré surface of section at  $B=1.4B_0$ . In constructing the Poincaré map, we keep the chaotic cavity open to retain the experimental situation. We inject a large number of electrons from the left-hand side lead. The values of  $v_x$  and  $x$  when the electrons cross the  $y=0$  line with  $v_y>0$  are indicated by the points. Consequently, true regular orbits do not show up in our plot. The phase space consists of stochastic seas and islands filled with periodic and quasiperiodic orbits. These so-called Kolmogorov-Arnol'd-Moser (KAM) orbits are stable and the existence of the islands is believed to be responsible for the power-law probability distributions [13]. When the cavity is formed by a hard wall, the probability of electrons pursuing

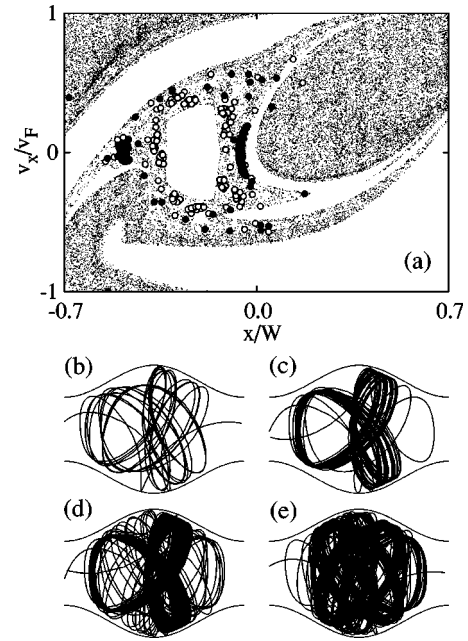


FIG. 2. (a) Poincaré surface of section at  $B=1.4B_0$ . The points represent  $v_x$  and  $x$  when a trajectory crosses the horizontal symmetry line with  $v_y>0$ . The contributions by the trajectories shown in (d) and (e) are indicated by the filled and open circles, respectively. The long trajectories with  $t/t_0=36, 88,$  and  $274$  that are shown, respectively, in (b)–(d) circulate in the vicinity of an identical orbit. The trajectory in (e), with  $t=358t_0$ , sticks to another regular orbit.

long trajectories typically diminishes exponentially. However, the electrons in the soft-wall cavity spend a long time in the vicinity of the stable orbits because of the stickiness of the hierarchical phase space structures. The dwell time becomes longer when the trajectories in the phase space stick closer to the KAM orbits [14]. The large dwell time of the trapped trajectories is essential for the power-law probability distributions.

Classical leads, in principle, couple with orbits in the cavity with a uniform probability. Therefore, the quantum-mechanical injection of electrons from a narrow lead was speculated in Ref. [8] to be the mechanism for a preferential excitation of a small number of regular orbits. However, the selective excitation of regular orbits takes place even with classical leads as incident electrons are trapped around these orbits, as we show below. As is evident in Figs. 2(b)–2(d), many long trajectories exhibit the same orbit pattern. Usually, several stable orbits are found to coexist when  $r_c>W$ . For example, the trajectory in Fig. 2(e) is trapped to another stable orbit. The regular orbit in Fig. 2(e) may be regarded as a mixture of the stable orbit in Fig. 2(d) and its mirror-reflected image with respect to  $x=0$ , which is also a stable orbit in the cavity. However, the Poincaré map reveals that the two trajectories are rather distinct stable orbits. In Fig. 2(a), the contributions by the trajectories shown in Figs. 2(d) and 2(e) are presented by the filled and open circles, respectively. Clearly, the two trajectories are attracted to different phase space structures.

We now turn our attention to the quantum transport properties in the cavity. Figure 3 shows the conductance of the cavity as a function of  $\hbar\omega_c/E_F$ , where  $\omega_c=eB/m$  is the cyclotron frequency. The conductance is related to the trans-

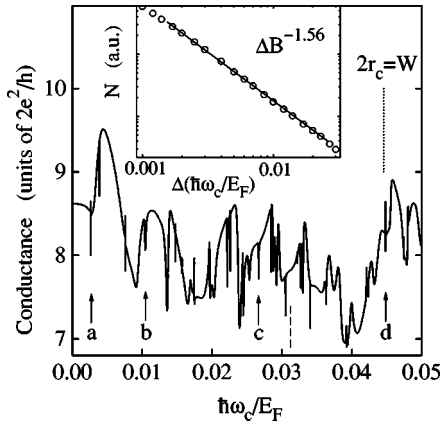


FIG. 3. Magnetoconductance of the soft-wall cavity when  $L = 20\lambda_F$ . The dashed and dotted lines indicate magnetic fields where  $B/B_0 = 1.4$  and 2, respectively. Inset: Fractal analysis of conductance fluctuations using a modified box-counting algorithm. The solid line manifests the power-law behavior, giving the fractal dimension  $D = 1.56$ .

mission probabilities between the leads by the Landauer formula. We have calculated the transmission probabilities using the lattice Green's function technique [15]. The cavity potential within a width of  $1.4W$  is simulated by a square lattice having 160 transverse lattice sites. The parabolic potential outside the cavity boundary defined by  $y_B$  is hence taken into account. The Fermi energy is chosen such that the lead contains 11 occupied modes.

The semiclassical theory of Ketzmerick [10] predicts that the conductance fluctuations are fractal when the probability distributions are given by a power law. As  $P(A)$  in Fig. 1 obeys a power law, the conductance fluctuations in Fig. 3 are expected to be fractal. We show the result of a modified box-counting analysis in the inset of Fig. 3. The number of "boxes"  $N$  is evaluated as follows. We divide the magnetic-field range with an interval  $\Delta(\hbar\omega_c/E_F)$ . The difference of the maximum and minimum conductance values within the interval is added over the segments. The sum divided by  $\Delta(\hbar\omega_c/E_F)$  is regarded as  $N$ . One indeed finds that the conductance fluctuations are fractal over at least one order of magnitude of  $B$ . (The lower bound might have been imposed by the limited number of data points.) The fractal behavior manifests that the tight-binding lattice is fine enough to examine the chaotic classical dynamics in the cavity. We obtain a fractal dimension  $D = 1.56$ . It has been derived that  $D$  is related to the power-law exponent of  $P(A)$  ( $\propto A^{-\beta}$ ) as  $D = 2 - \beta/2$  [10]. This relation expects the fractal dimension to be 1.2, which is considerably smaller than the value found in the quantum-mechanical calculation. In Ref. [11], a similar discrepancy was observed in a simulation using a square-like cavity. If the magnetic-field range for the fractal analysis is too wide, the classical dynamics may be fundamentally altered, resulting in a variation of  $\beta$  with the magnetic field, although the numerical result in Fig. 1 indicates that this is unlikely to be the case. To be confident about the estimate of  $D$ , we also carried out the fractal analysis using a restricted magnetic-field range. The fractal dimension was confirmed to be independent of the magnetic field. At present, the origin of the disagreement is not understood.

For the transmission resonances labeled a–d in Fig. 3, we

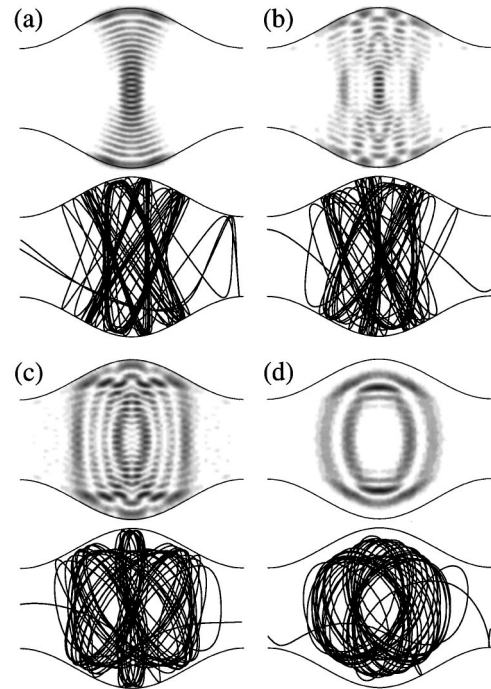


FIG. 4. Local density of states  $\rho(\mathbf{r})$  in the cavity shown in gray scale. (a)–(d) correspond to the transmission resonances labeled a–d in Fig. 3, respectively. A classical trajectory trapped to a stable orbit at each magnetic field is shown underneath.

show in Fig. 4 gray-scale plots of the local DOS

$$\rho(\mathbf{r}) = -\pi^{-1} \text{Im} G^+(\mathbf{r}, \mathbf{r}; E_F), \quad (2)$$

where  $G^+(E) = (E - H + i\epsilon)^{-1}$  is the retarded Green's function with  $H$  being the Hamiltonian of the system. Below the gray-scale plot, a typical long trajectory at each corresponding magnetic field is shown. The characteristic features in the quantum probability density and the stable orbit resemble each other with a remarkable accuracy. It is thus apparent that the wave-function pattern at the transmission resonance is closely associated with the underlying classical dynamics.

The correspondence may provide a semiclassical interpretation of the transmission resonance. In chaotic dynamics,  $P(A)$  is a smooth function of  $A$ . Hence, there is no special enclosed area that can explain the appearance of the transmission resonance at certain magnetic fields. However, the stable orbits may play an important role provided that long trajectories dominate the transport characteristics. It is suggested that the transmission resonance takes place when the stable orbit satisfies Bohr and Sommerfeld's (BS) quantization rule. Fromhold *et al.* [16] demonstrated that quantum numbers can be assigned to the scar patterns in resonant tunneling diodes using the quantization rule. The trajectories that follow a stable orbit with various revolutions satisfy the BS quantization condition simultaneously. The quantum interference effects will lead to a profound influence of the stable orbits in determining the conductance. We note that the width of the transmission resonance is given by the strength of the coupling between the states in the cavity and the lead, and so it depends on the position of the leads with respect to the stable orbit [1].

Due to the symmetric cavity geometry, the quantum eigenstate pattern in our system has to fulfill the symmetry. Therefore, it may seem that asymmetric stable orbits, like the one in Fig. 2(d), do not give rise to a scarlike feature. However, a quantum eigenstate can be produced by a superposition of the asymmetric stable orbit and all of its mirror reflections as all the orbits satisfy the BS quantization rule at the same time.

Our result supports the idea proposed by Markus *et al.* [5] that the wave-function scarring and the quasiperiodic conductance fluctuations have a common origin. As the probability density reveals pronounced scarring only at transmission resonances, it was argued by Zozoulenko *et al.* [9,17] that the scarring is unlikely to cause the quasiperiodicity. However, as the scarlike feature arises from the stable orbits of the underlying classical dynamics, its implication is not restricted to some magnetic fields. Moreover, the stable orbits vary with magnetic field rather gradually, and so the BS quantization rule is fulfilled in a fairly periodic manner.

When the probability distribution decays exponentially, all regular orbits are unstable and there are no KAM islands [13]. Hence, the regular orbits in hard-wall cavities are usually unable to trap electrons that pass around them. (A power law can be realized in some hard-wall cavities as shown by the dotted line in Fig. 1.) Most of the numerical studies of the cavity conductance reported so far [6,8,9] assumed hard-wall confinements. This is probably the reason that the scarring in square [6,9] and stadium-shaped [8,18] cavities was observed only in relatively high magnetic fields. In particular, without a substantial smooth potential, the probability distributions in squarelike cavities are rigidly exponential. By applying a magnetic field, the probability distributions can be transformed from an exponential behavior to a power-law behavior [12]. The scarring found in Refs. [8] and [9] may originate from the trapping to hierarchical phase space structures induced by the magnetic field. In our system, well-developed scarlike patterns are found for all the transmission resonances, and they are unambiguously identified with the stable orbits. In fact, the scarlike features can be recognized even for magnetic fields away from the resonance. In analyzing conductance fluctuations to compare with experiments, one has to clarify whether the classical dynamics induces the power-law or the exponential probability distribution.

In classical dynamics, only a small portion of incident electrons travel along the long trajectories. In addition, the probability for these electrons to exit the cavity through a particular lead barely changes with a small change in  $B$ .

Therefore, the stable orbits produce a background variation, and the influence of the characteristic phase space structures of chaotic dynamics is negligible in the billiard model [19]. The phase space structures have been assumed to be the origin of hierarchical repetitions of magnetoconductance fluctuations that were observed experimentally in Sinai billiards [20]. However, no theory has succeeded in reproducing the experimental finding [11]. We emphasize that soft boundary potentials are inevitable in devices defined by Schottky gates. Instead of the hierarchical phase space structures, stable orbits that may have resulted from the soft confinement and/or the magnetic field might provide an explanation for the self-similar fluctuations.

In high magnetic fields, both the local DOS and the stable orbit show a circular pattern. High-magnetic-field measurements of the conductance are often used to infer the cavity size. The interpretation of the edge state as an orbit skipping along the boundary is readily justified when  $r_c$  is much smaller than the cavity size. Our simulation indicates that the edge state is established in a soft-wall cavity even when the magnetic field is not very high. Therefore, the onset of Aharonov-Bohm (AB) conductance oscillations can be significantly lower than expected in the skipping orbit picture. In our cavity geometry, the stable orbit bears a loop shape for  $B \geq 2B_0$ . We find that the area covered by the chaotic trajectories in this regime is nearly independent of the magnetic field, although it is slightly extended toward the leads in high fields. Thus, the period of the AB oscillation is expected to depend rather weakly on the magnetic field.

In conclusion, we have investigated chaotic trajectories and wave functions in a cavity defined by a smooth confinement potential. The underlying classical dynamics selects a few regular orbits, to which long trajectories are trapped. The characteristic pattern of the wave function at quantum transmission resonances is found to be identical to these stable orbits, resolving the question of which regular orbit is chosen as the scarlike pattern of a transmission resonance. The exact match evidences the self-control of the cavity dynamics, which is in contrast to the popular view that it is driven by the leads. The correspondence allows us to interpret the quasiperiodicity of magnetoconductance fluctuations in ballistic cavities in terms of the stable orbits rather than the scarring. As the stable orbits are present irrespective of the magnetic-field value, the interpretation based on classical dynamics is applicable to a wider range of issues in comparison to the scarring effect.

- 
- [1] Y. Takagaki and D.K. Ferry, *J. Phys.: Condens. Matter* **5**, 1975 (1993).  
 [2] E.J. Heller, *Phys. Rev. Lett.* **53**, 1515 (1984).  
 [3] L. Kaplan and E.J. Heller, *Ann. Phys. (N.Y.)* **264**, 171 (1998).  
 [4] S. Tomosovic and E.J. Heller, *Phys. Rev. Lett.* **70**, 1405 (1993); O. Agam and S. Fishman, *ibid.* **73**, 806 (1994); L. Kaplan, *ibid.* **80**, 2582 (1998).  
 [5] C.M. Markus, A.J. Rimberg, R.M. Westervelt, P.F. Hopkins, and A.C. Gossard, *Phys. Rev. Lett.* **69**, 506 (1992).  
 [6] J.P. Bird, R. Akis, D.K. Ferry, Y. Aoyagi, and T. Sugano, *J. Phys.: Condens. Matter* **9**, 5935 (1997).  
 [7] J.P. Bird, R. Akis, D.K. Ferry, D. Vasileska, J. Cooper, Y. Aoyagi, and T. Sugano, *Phys. Rev. Lett.* **82**, 4691 (1999).  
 [8] R. Akis, D.K. Ferry, and J.P. Bird, *Phys. Rev. Lett.* **79**, 123 (1997); R. Akis, D.K. Ferry, J.P. Bird, and D. Vasileska, *Phys. Rev. B* **60**, 2680 (1999).  
 [9] I.V. Zozoulenko, R. Schuster, K.-F. Berggren, and K. Ensslin, *Phys. Rev. B* **55**, 10 209 (1997); I.V. Zozoulenko and K.-F. Berggren, *ibid.* **56**, 6931 (1997).  
 [10] R. Ketzmerick, *Phys. Rev. E* (to be published).  
 [11] Y. Takagaki and K.H. Ploog, *Phys. Rev. B* **61**, 4457 (2000).  
 [12] Y. Takagaki, M. ElHassan, A. Shailos, C. Prasad, J.P. Bird,

- D.K. Ferry, K.H. Ploog, L.-H. Lin, N. Aoki, and Y. Ochiai, Phys. Rev. B (to be published).
- [13] J.D. Meiss and E. Ott, Phys. Rev. Lett. **55**, 2741 (1985).
- [14] G.M. Zaslavsky, D. Stevens, and H. Weitzner, Phys. Rev. E **48**, 1683 (1993).
- [15] D.S. Fisher and P.A. Lee, Phys. Rev. B **23**, 6851 (1981); T. Ando, *ibid.* **44**, 8017 (1991).
- [16] T.M. Fromhold, P.B. Wilkinson, F.W. Sheard, L. Eaves, J. Miao, and G. Edwards, Phys. Rev. Lett. **75**, 1142 (1995).
- [17] I.V. Zozoulenko and T. Lundberg, Phys. Rev. Lett. **81**, 1744 (1998).
- [18] K. Nakamura and H. Ishio, J. Phys. Soc. Jpn. **61**, 3939 (1992).
- [19] C.W.J. Beenakker and H. van Houten, Phys. Rev. Lett. **63**, 1857 (1989); M.L. Roukes and O.L. Alerhand, *ibid.* **65**, 1651 (1990).
- [20] R.P. Taylor, R. Newbury, A.S. Sachrajda, Y. Feng, P.T. Coleridge, C. Dettmann, N. Zhu, H. Guo, A. Delage, P.J. Kelly, and Z. Wasilewski, Phys. Rev. Lett. **78**, 1952 (1997).